TECHNIUM
SOCIAL SCIENCES JOURNAL

Technium.

40/2023

2023

A new decade for social changes

Technium Social Sciences

Powered by PLUS COMMUNICATION
International Communication & PR

Technium Social Sciences Journal
Vol. 40, 529-537, February, 2023
ISSN: 2668-7798
www.techniumscience.com

The behaviour of a retaining wall under seismic excitation

Tounsia Boudina[1], Sofiane Bounouni[1], Aicha Rouabeh[2], Naas Allout[3]

[1]Architecture department, University of Bejaia, 06000 Bejaia – Algeria. [2]Civil engineering department, University of Bouira, Algeria, [3]Civil engineering department, Zian Achor University, Djelfa– Algeria.

tounsia.boudina@univ-bejaia.dz, sofiane.bounouni@univ-bejaia.dz , aicha.rouabeh@univ-bouira.dz, allout.naas@univ-djelfa.dz

Abstract. In this research, the different methods to calculate the earth pressures on a retaining wall were exposed, for different loading conditions, namely static and dynamic. The dynamic response of a retaining wall under seismic loading was also studied. The simulation is done using the finite element code PLAXIS. The response is expressed in terms of acceleration and displacement. When using numerical models to study this type of problem, two different entities can be identified. The first one corresponds to the materials and the consideration of their behavior. The second part corresponds to the type of loading imposed, i.e. the input signal.

Keywords. retaining wall, seismic loading, behavior, permanent displacement.

1. Introduction

In this paper, we study the response of a retaining wall during an earthquake. We also study the influence of the frequency content of the seismic and amax motion as well as the importance of taking into account the behavior of the backfill soil on the permanent displacement of the wall.

2. Numerical modeling

The finite element model is shown in figure 1. It is 160 m wide and 20 m high, in order to place the lateral boundaries far enough away. This should help to reduce the influence of the boundaries on the results obtained, although there is no clear indication in the literature on this aspect. Recently, various research [1] showed a case of site response analysis in which they kept the width of the model eight times its height, in order to obtain acceptable results.

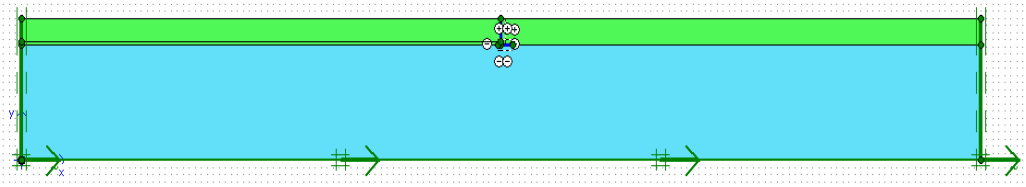

Figure 1. Finite element model used in dynamic analysis.

Technium Social Sciences Journal
Vol. 40, 529-537, February, 2023
ISSN: 2668-7798
www.techniumscience.com

The soil is schematized as an elasto-plastic layer which is implemented in the Plaxis code. Its parameters are shown in table 1.

Table 1. Properties of the soil layers.

Soil layers	Model used	γ (KN/m³)	E (KN/m²)	ν	φ(°)	C (KN/m²)
Clay 1	Mohr-Coulomb	20.4	4.43E+05	0.3	21.8	100
Clay 2	Mohr-Coulomb	20.0	3.66E+05	0.3	30	20

The wall is idealized using an elastic "flat" element. Its properties are summarized in the table 2.

Table 2. Properties of the elements constituting the retaining wall.

Structures used	Model used	EA	EI	ν
Wall	linear elastic	3.10E+07	1.95E+05	0.2
Sole	linear elastic	2.51E+07	1.88E+05	0.2

The soil-structure friction is simulated with an interface element characterized by the imposed R_{inter} parameter equal to :

$$R_{inter} = \frac{tg\delta}{tg\phi} = 0.67 \qquad (1)$$

The generation of the mesh in PLAXIS is fully automatic and is based on a valid triangulation procedure, which results in an "unstructured" mesh. In the meshes used in the current analyses, the basic type of elements is the 15-node triangular element. The dimensions of any triangle can be controlled by the local height of the element.

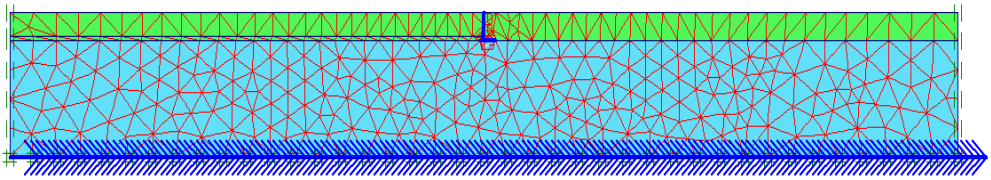

Figure 2. Discretization of the model studied by triangular elements of 15 nodes

3. Calibration of the numerical model

Before any dynamic analysis is performed, it is necessary to make some consideration about some critical points in the modeling. The calibration of the numerical model is required to reduce the influence of some parameters on the final results. In a dynamic finite element analysis different sources of energy dissipation exist: material damping which includes viscous and hysteresis damping of the soil, numerical damping, resulting from the adopted integration scheme and energy dissipation at the boundaries which is presented by the way the numerical model transmits wave energy outside the domain [2]. In most FE dynamic codes, such viscous damping is simulated according to the well-known Rayleigh formulation. The damping matrix **C** is assumed to be proportional to the mass matrix **M** and the stiffness matrix **K** by means of two coefficients, αR and βR as follows:

$$C = \alpha_R M + \beta_R K \qquad (2)$$

Technium Social Sciences Journal
Vol. 40, 529-537, February, 2023
ISSN: 2668-7798
www.techniumscience.com

There are different criteria for evaluating Rayleigh coefficients [3-5]. The dynamic response of a system is significantly affected by the choice of these parameters.

In the PLAXIS code, the Rayleigh damping formulation is implemented and the values of α_R and β_R can be estimated by the following system of equations:

$$\alpha_R + \beta_R \omega_m^2 = 2\omega_m \xi \quad (3)$$

$$\alpha_R + \beta_R \omega_n^2 = 2\omega_n \xi \quad (4)$$

Such that ξ is the accepted value for the damping constant, ω_m and ω_n are two fundamental angular frequencies of the ground related to the frequency interval ($fm \div fn$) over which the viscous damping is less than or equal to ξ.

The values of α_R and β_R are summarized in the following table:

Table 3. The values of the Rayleigh coefficients α_R and β_R.

Layers	ω_m (rad/s)	ω_n (rad/s)	ξ	α_R	β_R
Clay1	2.7646015	24.881414	0.05	1.685	0.00111
Clay2	5.8645077	29.322538	0.05	1.547	0.00121

In the numerical execution of dynamic problems, the formulation of the time integration algorithm is an important factor for the stability and accuracy of the computational process. Explicit and implicit integration are two commonly used strategies for time integration. In the Plaxis 2d v.8.2 code [6], the implicit time integration strategy of Newmark type is implemented. In this method, the displacement and velocity of any point at time t+Δt are expressed as.

$$u^{t+\Delta t} = u^t + \dot{u}^t \Delta t + \left[\left(\frac{1}{2} - \alpha_N\right)\ddot{u}^t + \alpha_N \ddot{u}^{t+\Delta t}\right]\Delta t^2 \quad (5)$$

$$\dot{u}^{t+\Delta t} = \dot{u}^t + [(1-\beta_N)\ddot{u}^t + \beta_N \ddot{u}^{t+\Delta t}]\Delta t \quad (6)$$

The coefficients α_N and β_N control the accuracy of the numerical time integration. They define the variation of the acceleration response in each time step and determine the stability of these methods. They are expressed as a function of the parameter γ [7].

$$\alpha_N = \frac{(1+\gamma)^2}{4} \quad (7)$$

$$\beta_N = \frac{1}{2} + \gamma \quad (8)$$

Where the value of γ belongs to the interval [0, 1/3].

Since we adopted the standard values in PLAXIS of the Newmark coefficients α_N=0.3025 and β_N=0.6 which corresponds to γ=0.1>0. Therefore, the values of β_R must be reduced by the quantity γdt, where dt is the time step.

The time step used in the dynamic calculation is constant and equal to:

$$dt = \Delta t/(n \times m) \quad (9)$$

Where Δt is the duration of the dynamic loading (Time interval), n is the number of additional steps (Additional steps) and m is the number of dynamic sub steps (Dynamic sub steps).

The choice of boundary conditions affects the amount of energy dissipation due to wave propagation in the ground. The position of the boundary and the type of mechanical fixtures should reproduce, as best as possible, the energy transmission outside the computational domain.

Technium Social Sciences Journal
Vol. 40, 529-537, February, 2023
ISSN: 2668-7798
www.techniumscience.com

Viscous absorbing boundaries based on the method described by Lysmer and Kuhlemeyer (1969) [8] are the most widely used procedures. In this case, the normal and tangential components of the absorbed stresses at the boundary are:

$$\sigma_n = -c_1 \rho v_P \dot{u}_n \quad (10)$$

$$\tau = -c_2 \rho v_S \dot{u}_t \quad (11)$$

Where ρ is the density of the material, v_P and v_S are the compressional and shear wave velocities, $\dot{u}_n$and $\dot{u}_t$ are the normal and tangential velocity components, c_1 and c_2 are the relaxation coefficients. Some suggestions exist in the literature for the choice of these parameters. A recent study shows that no significant difference was identified in the numerical results by adopting different values of these parameters in the range 0÷1 [9]. We adopted the standard values in PLAXIS of the relaxation coefficients c_1=1 and c_2=0.25.

4. Dynamic analysis

The problem analysis was performed in 4 computational phases (3 plastics and 1 dynamic analysis). From phase 1 to phase 3 the excavation was performed deactivating the layers next to the wall. Phase 4 was devoted to define the acceleration imposed on the base of the model, we are only interested in the propagation of shear waves SH, therefore, the input signal is considered parallel to the base and we do not take into account the vertical component of the movement.

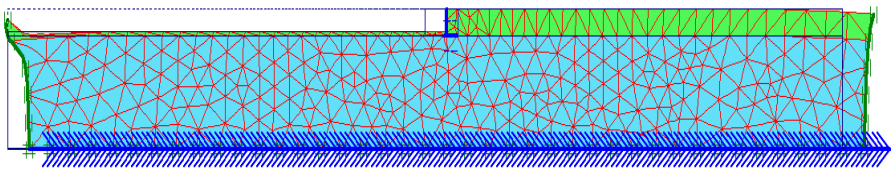

Figure 3. The deformation of the model after the dynamic analysis.

In order to study the seismic response of the retaining wall, we are interested in the response at five representative points in the model. The first point is located at the top of the wall (point A). The second point is located at the base of the wall (point B). The third point is located at the surface of the natural terrain (after excavation) and is 20m downstream of the retaining wall (point C). The fourth point is located at the surface of the embankment (point D). The last point is located at the base of the embankment at a distance of 20m from the wall (point E) also at a distance of 20m upstream from the wall.

Figures (4) to (8) show the accelerations obtained in the five selected points. The input signal corresponds to the Boumerdes earthquake (Keddara1 E-W) with a maximum acceleration a_{max} = 0.33g.

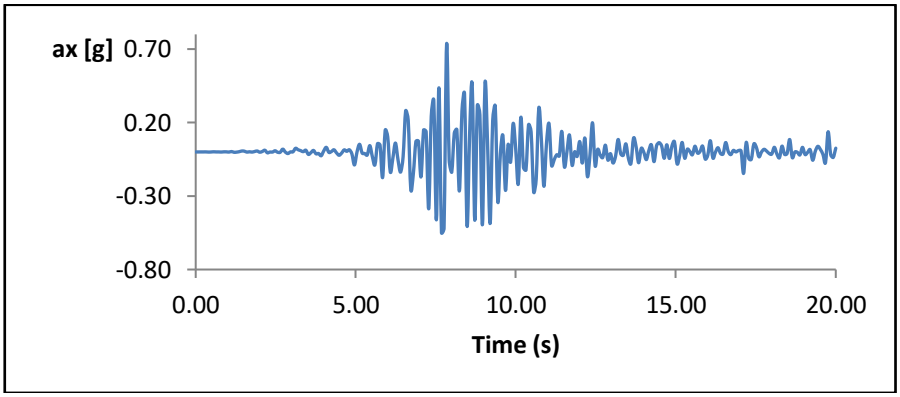

Technium Social Sciences Journal
Vol. 40, 529-537, February, 2023
ISSN: 2668-7798
www.techniumscience.com

Figure 4. Acceleration versus time at point A (top of the wall).

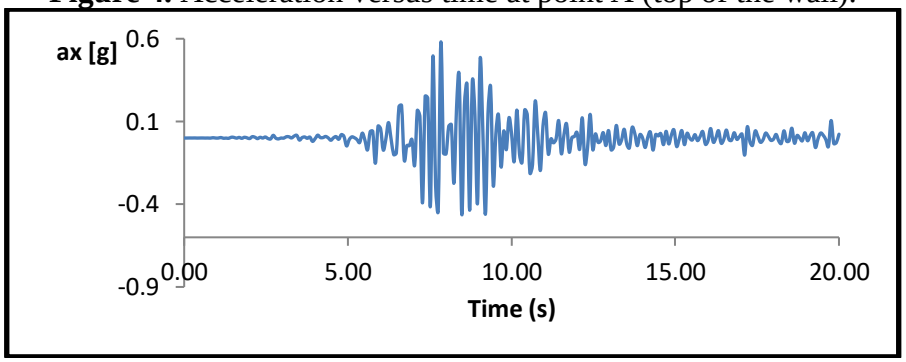

Figure 5. Acceleration versus time at point B (base of the wall).

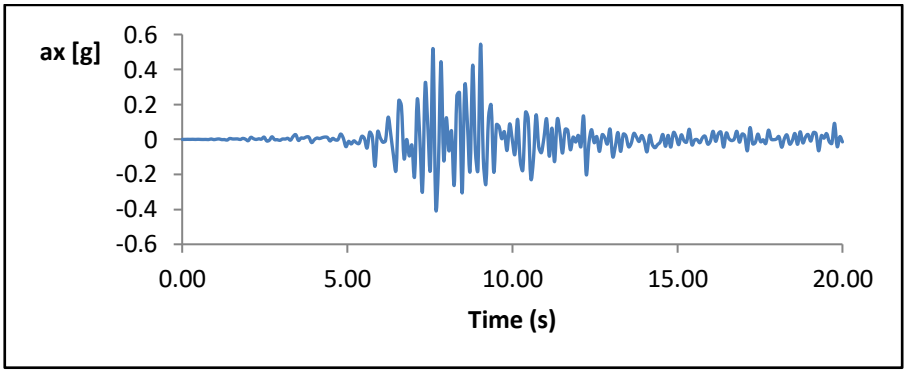

Figure 6. Acceleration versus time at point C (base of the embankment).

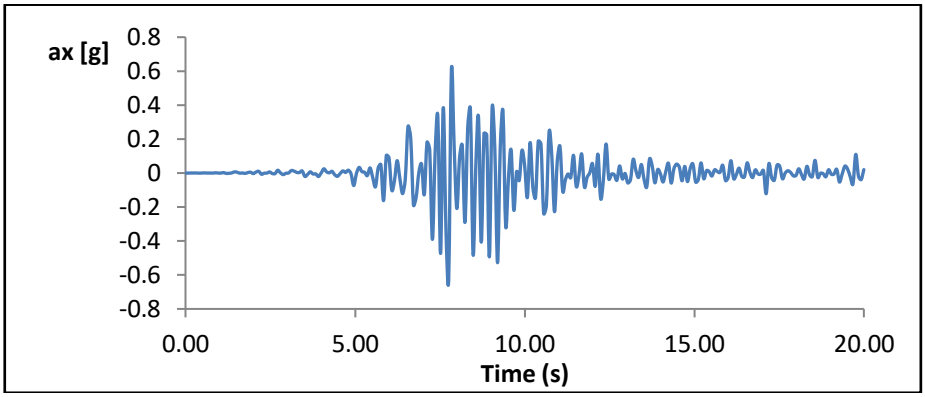

Figure 7. Acceleration versus time at point D (downstream of the wall).

Technium Social Sciences Journal
Vol. 40, 529-537, February, 2023
ISSN: 2668-7798
www.techniumscience.com

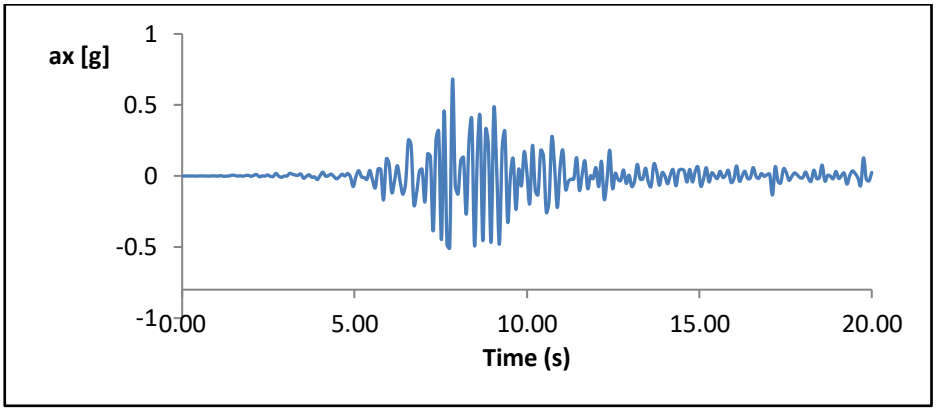

Figure 8. Acceleration versus time at point E (upstream of the wall).

Now, the influence of the consolidation state of the embankment soil on the value of the maximum acceleration at the base of the a_{maxE} embankment is studied. For this purpose, we compare the responses obtained for the proposed model at three a_{maxbed} levels of the Boumerdes earthquake (Table 4).

Table 4. Comparison of a_{max} values at point E for embankments R1 (normally-consolidated) and R2 (over-consolidated).

	Soil R_1	**Soil R_2**
a_{maxbed} **(g)**	a_{maxE} **(g)**	a_{maxE} **(g)**
0.33	0.65	0.68
0.40	0.68	0.70
0.50	0.71	0.78

From the table above, it can be seen that the maximum acceleration values obtained using the two models (R1 and R2) are approximately the same.

5. Induced displacement calculation

This section focuses on the influence of the embankment soil behavior and the input signal on the value of the permanent displacement of the retaining wall during dynamic loading. The displacements of the U_A wall correspond to the displacements obtained at the top of the wall.

5.1. Influence of the behaviour of the backfill soil

In this subsection, the influence of taking into account the dilatant or contracting behavior of the backfill soil on the value of the displacement of the retaining wall is studied. For this purpose, we only change their consolidation state. Thus, the embankment (R_1) is normally consolidated (OCR=1) and the second (R_2) is over-consolidated (OCR=2).

A comparison of the responses of embankments R_1 and R_2 for the same conditions was made. Figure 9. shows the response of the two embankments to the Boumerdes earthquake (Keddara1E-W) with a maximum acceleration at the rock a_{maxbed} = 0.33g.

Technium Social Sciences Journal
Vol. 40, 529-537, February, 2023
ISSN: 2668-7798
www.techniumscience.com

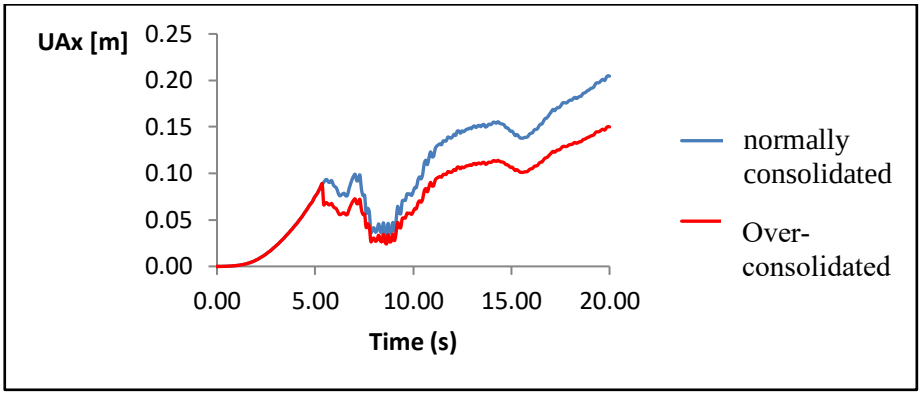

Figure 9. Displdisplacements obtained for normally consolidated and over consolidated fill soils for the same value of a_{max}.

According to this figure, the displacements obtained for embankment R_1 (contracting behavior) are larger than those obtained by the model with embankment R_2 (expanding behavior).

5.2. Influence of the input signal

To study the influence of the input signal on the rock. We first study the effect of the amplitude (i.e. the value of the maximum acceleration a_{max}) and then the effect of the frequency content of the signal (i.e. average period T_m).

Figure (10) shows the comparison of horizontal displacements U_{AX} obtained for the proposed model subjected to three levels of a_{max} of the Boumerdes earthquake (Keddara1 E-W) As expected, a larger displacement is obtained when the level of acceleration a_{max} of the input signal is greater.

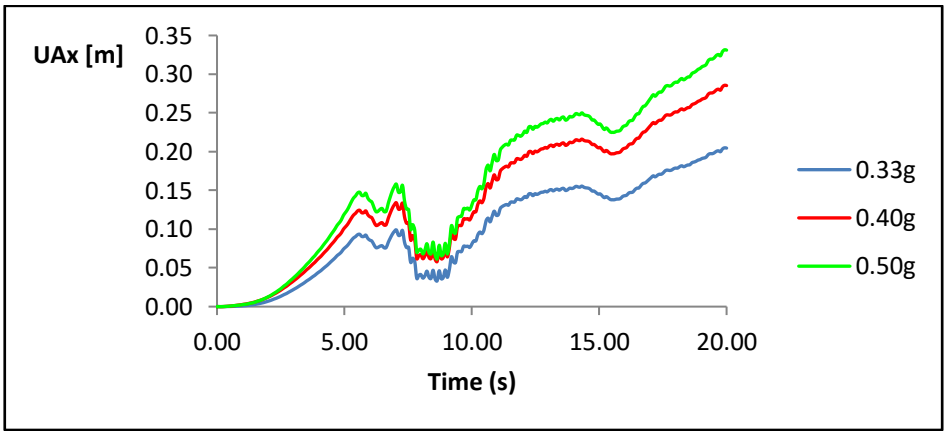

Figure 10. Displacements as a function of time, at point A, obtained for three levels of a_{max}.

The values of the displacements obtained are summarized in the following table:

Table 5. Values of horizontal displacements at point A, obtained for three levels of a_{max}.

Acceleration at the base of the model	Displacement U_{AX} *(cm)*
0.33g	20.49
0.40g	28.56
0.50g	33.15

Technium Social Sciences Journal
Vol. 40, 529-537, February, 2023
ISSN: 2668-7798
www.techniumscience.com

Now, if we look at the vertical displacements U_{AY} or wall settlements (Table 6), we can see from the results that the value of U_{AY} also increases with the acceleration level of the input signal.

Table 6. Values of vertical displacements at point A, obtained for three levels of a_{max}.

Acceleration at the base of the model	Displacement U_{AY} (cm)
0.33g	2.69
0.40g	3.08
0.50g	3.79

In order to study the influence of the frequency content of the input signal on the displacement of the wall, various signals with the same level of acceleration to the rock have been imposed on the proposed model. For this we used the signals of Dar El-Beida and Hussein Dey "scaled" to 0.33g.

The displacements obtained are presented in the table 7.

Table 7. Displacement values obtained for various signals

Station	$a_{max\ bed}$ (g)	T_m (s)	a_{maxE} (g)	T_m (s)	U_{AX} (cm)
Kedarra	0.33	0.199	0.68	0.195	20.50
Dar El-Beida	0.33	0.389	0.62	0.207	07.04
Hussein-Dey	0.33	0.590	0.40	0.244	13.73

If we compare the displacement values obtained, we see that the displacements vary according to the signal used. However, this variation is not directly related with the variation of the value of Tm of the earthquakes. We also notice that, although the value of the maximum acceleration at the amaxC embankment is not the same for the three signals used, it is not the only cause of the difference in the displacement values of the wall.

6. Conclusion

From the different results obtained, it can be seen that the failure mechanism for the proposed model is that of sliding failure (Translation), i.e., the wall slides away from its base (Figure 3). With this type of failure, the wall moves away from the embankment.The substitution of sand by waste brick aggregates, causes a slight loss of consistency of the pastes, due to the adsorptive character of calcined clays.

From these results, it can be concluded that the maximum acceleration values obtained using the two embankment consolidation states (R_1: normally consolidated and R_2: overconsolidated) are very similar and therefore the effect of the dilatant behavior of the embankment soil on the $a_{max}C$ value can be neglected. Therefore, the value of the signal acceleration at the base of the embankment is little influenced by the behavior of the embankment soil. However, this behavior does influence the displacements of the foundation soil.

Finally, we notice that the horizontal displacements of the wall are important. This is of course due to the amplification of the acceleration at the base of the embankment, produced for

the presence of the foundation soil. This result highlights the importance of taking into account the "site effect" of the foundation soil on the level of acceleration that arrives at the base of the wall.

References

[1] XIAOYONG ZHANG, TIANCHENG WANG and GUOXIONG MEI: "Supporting mechanism of rigid-flexible composition retaining structure in sand ground using discrete element method", Computers and Geotechnics, 12 August 2022, (2022).
[2] VISONE.C: "Performance-Based Approach In Seismic Design Of Embedded Retaining Walls", Università Degli Studi Di Napoli Federico Ii Polo Delle Scienze E Delle Tecnologi Dottorato Di Ricerca In Rischio Sismico Xxi Ciclo, (2008).
[3] HASHASH.Y.M. A AND PARK.D: "Viscous damping formulation and high frequency motion propagation in non-linear site response analysis", Soil Dynamics and Earthquake Engineering 22 (2002) 611–624, (2002).
[4] LANZO G., PAGLIAROLI A., D'ELIA B:" L'influenza della modellazione di Rayleigh dello smorzamento viscoso nelle analisi di risposta sismica locale", ANIDIS, XI Congresso Nazionale "L'Ingegneria Sismica in Italia", Genova 25-29 (in Italian), (2004).
[5] PARK.D AND HASHASH.Y.M. A: "Soil Damping Formulation In Nonlinear Time Domain Site Response Analysis", Journal of Earthquake Engineering, Vol. 8, No. 2, 249-274, (2004).
[6] YAN YU, IVAN P. DAMIANS, RICHARD J. BATHURST: " Influence of choice of FLAC and PLAXIS interface models on reinforced soil–structure interactions" Computers and Geotechnics, April 2015, (2015).
[7] VISONE.C, EMILIO.B: "Comparative Study on Frequency and Time Domain, (2010).
[8] BUND. A: Analyses for Seismic Site Response", EJGE, Vol. 15,
[9] KUHLEMEYER.R. L AND LYSMER.J: "Finite element method accuracy for wave propagation problems", Journal of the Soil Mechanics and Foundations Division, ASCE, Vol. 99, No. SM5, pp. 421-427, (1969).
[10] RITWIK NANDI and DEEPANKAR CHOUDHURY: "Displacement-controlled approach for the analysis of embedded cantilever retaining walls with a distanced strip surcharge", Computers and Geotechnics, 19 August 2022. (2022).